ELECTRICAL RESISTANCE AND THERMOELECTRIC POWER OF THE METASTABLE PHASES IN TELLURIUM-BASE ALLOYS

Thesis by

Chang-chyi Tsuei

In Partial Fulfillment of the Requirements
For the Degree of
Doctor of Philosophy

California Institute of Technology

Pasadena, California

1966

(Submitted May 26, 1966)

TO MY PARENTS

ACKNOWLEDGMENT

The author wishes to express his gratitude to Professor P. Duwez for his valuable advice and tireless encouragement throughout this work. He also thanks Professors F. S. Buffington and R. H. Willens for their reading of the manuscript and many helpful suggestions.

ABSTRACT

By using techniques of rapid quenching from the melt, metastable phases have been obtained in ternary alloys which contain tellurium as a major component and two of the three noble metals (Cu, Ag, Au) as minor components. The metastable phases found in this investigation are either simple cubic or amorphous. The formation of the simple cubic phase is discussed. The electrical resistance and the thermoelectric power of the simple cubic alloy (Au_{30} Te_{70}) have been measured and interpreted in terms of atomic bondings. The semiconducting properties of a metastable amorphous alloy (Au_5 Cu_{25} Te_{70}) have been measured. The experimental results are discussed in connection with a theoretical consideration of the validity of band theory in an amorphous solid. The existence of extrinsic conduction in an amorphous semiconductor is suggested by the result of electrical resistance and thermoelectric power measurements.

TABLE OF CONTENTS

I. INTRODUCTION

Metastable phases in alloys always provide metallurgists, both theoretical and experimental, with many interesting properties. Many of them find important practical application in engineering. Martensite and precipitation hardened aluminum alloys are only two prominent examples. Traditionally, metastable phases have been obtained by quenching the alloy from the solid state. In this investigation, a recently developed technique[1] for rapid quenching alloys from the liquid state has been used to obtain metastable phases in ternary alloys which contain tellurium as a major component and two of the three noble metals as minor components. Metastable phases have been reported in Te-base binary alloys.[2], [3] The metastable phases found in this investigation are simple cubic and amorphous.

This thesis is mainly concerned with the electrical properties of the amorphous alloys. An amorphous material can be defined as a material which does not possess the long-range translational symmetry. This definition, however, does not prevent an amorphous material from having short-range order (coordination number and the average atomic distance). Therefore, the lack of long-range crystalline order does not necessarily mean an absolutely random atomic arrangement. In this work, our attention will be limited to amorphous solids only. It may be appropriate to point out that the distinction between an amorphous solid and a liquid lies in the fact that the atomic distribution of the latter is a complicate function of time while in the former it

does not vary with time if the thermal vibrations are neglected. Therefore, a knowledge of the properties of amorphous solids can serve as a stepping stone toward the understanding of the liquid state.

The application of quantum mechanics to solids in the crystalline state results in the "band theory" of solids which successfully explains many properties of metals, semiconductors and insulators. The energy band picture for electrons in a solid is a direct consequence of the quantum mechanical calculation of the motion of an electron in a periodic, self-consistent field. This one-electron approximation is essentially based on the periodicity of solids, so it is hard to reconcile the above concept with the experimental observation that many substances retain their characteristics of electrical conductivity on melting. Numerous experiments on metals and semiconductors have shown that the basic feature of the band structure changes little on the transition from the crystalline state to the liquid state or the amorphous state provided that the short-range order is not altered on transition. This seems to suggest that the short-range order plays a decisive role in determining the nature of band structure. The applicability of "band theory" goes far beyond the limits imposed by the periodicity of atomic arrangement from which it was deduced.

The semiconducting properties of a metastable amorphous alloy (Au_5 Cu_{25} Te_{70}) were measured and will be discussed in connection with a theoretical consideration of the validity of band theory in an amorphous solid.

Another interesting (and baffling) aspect of the semiconducting properties of an amorphous substance is the absence of impurity conduction. A number of vitreous semiconductors of various compositions were investigated[4] over a wide range of temperature. None of them showed the existence of impurity conduction. Introduction into such glasses of impurities which were found to be electrically active in crystals did not affect the electrical conductivity. This is a unique phenomenon of amorphous semiconductors. Several investigators[5], [6] have tackled this problem theoretically, but no conclusive result has been reached yet. This work will deal with the impurity effect in the amorphous alloy (Au_5 Cu_{25} Te_{70}) and present a possible evidence for the existence of extrinsic conduction in an amorphous solid. Thermoelectric properties of the amorphous alloy will also be discussed.

II. EXPERIMENTAL DESCRIPTION

A. Alloy Preparation

In this investigation, ternary alloys with tellurium as a major component are investigated. Each alloy contains tellurium and two of the three noble metals copper, silver and gold.

The source of supply and the purity of the elements used in this study are shown as follows:

Elements	Source of Supply	Specified Purity
Te	American Smelting & Refining Co.	99.999 + % Te, Mg, 1; Si 1; Fe, 1; Cu 1; ppm
Cu	Johnson Matthey & Co.	99.99% Cu; Fe 2; Pb 2; Ni 1; Ag 1; Cd, Mg, Mn Si, 1 ppm
Ag	Englehard Industry Inc.	99.99% Ag
Au	Wildberg Bros. Smelting & Refining Co.	99.99% Au

The alloys were prepared by induction-melting appropriate quantities of the component elements in a quartz crucible in an argon atmosphere. After reweighing, the alloys were cast into 1 mm wires. The weight loss is restricted to less than 0.2% to ensure good accuracy in alloy composition.

B. Quenching Technique

The details of the rapid quenching technique developed by

Duwez and Willens have been described in reference (1). The basic principle of this technique is to remove the heat from a small amount of molten alloy by conduction rather than by the conventional method through the heat transfer of a thin layer of vapor. Small portions (~20 mg) of the alloy wire were seated in the center of a vertical graphite crucible and melted by induction heating. The surface tension of the molten specimen keeps it from dropping through the small opening at the end of the crucible. This globule of liquid alloy is then ejected onto a polished copper strip and solidifies into a well-spread foil which is irregular in shape and non-uniform in thickness (~ 10 μ). For convenience in performing electrical measurements, the stationary copper target used in this experiment is straight and not bent as described in reference (1).

In the quenching process the target is kept in air and at room temperature. The specimen is protected by an argon atmosphere during heating.

C. X-Ray Diffraction

Two x-ray diffraction techniques are used in this work: the Debye-Scherrer method and the diffractometer method. The former is used to determine the lattice parameter and to identify the alloy structure; the latter is used only for the purpose of phase identification.

The Debye-Scherrer powder specimen is prepared by grinding the rapid-quenched alloy scraped from the copper substrate and packing it into a thin-walled capillary of 0.5 mm diameter. Then the capillary is mounted and centered in a Debye-Scherrer camera

(114.6 mm dia.). Typical exposure is about 4 hrs at 45 KV and 20 Ma with Ni filtered copper radiation. Exposed films are developed according to a standard procedure recommended by the film manufacturer. Correction is made for film shrinkage. The lattice parameter and its estimated uncertainty are determined by extrapolation against the Nilson-Riley function.

The diffractometer specimen is prepared by pouring a resin ("Quick Mount", a self-setting resin made by Fulton Metallurgical Products Corporation) into a Teflon mold placed over a specimen rapid-quenched on copper substrate. After the "Quick Mount" resin is allowed to set about 20 minutes or more, the quenched sample can be taken off the copper strip and is thus cast onto the surface of the resin mounting. No reaction has been observed between the quenched alloys and the resin. The cast sample is then mounted in a diffractometer to have its phase (or phases) identified. All the specimens were checked by the x-ray diffraction method prior to the electrical measurements.

D. Resistance Measurement

In order to facilitate the resistance measurement the rapid quenched sample is transferred to the surface of a "Quick Mount" resin mounting in the manner described in the last paragraph. Then the sample is machined into the appropriate shape as shown in Figure 1. The contact between the copper electrical lead and the specimen is of pressure type as shown in Figure 1. The specimen is then put into an aluminum container 6 $\frac{1}{2}$" high. 3" outside diameter and 1 $\frac{1}{2}$" inside

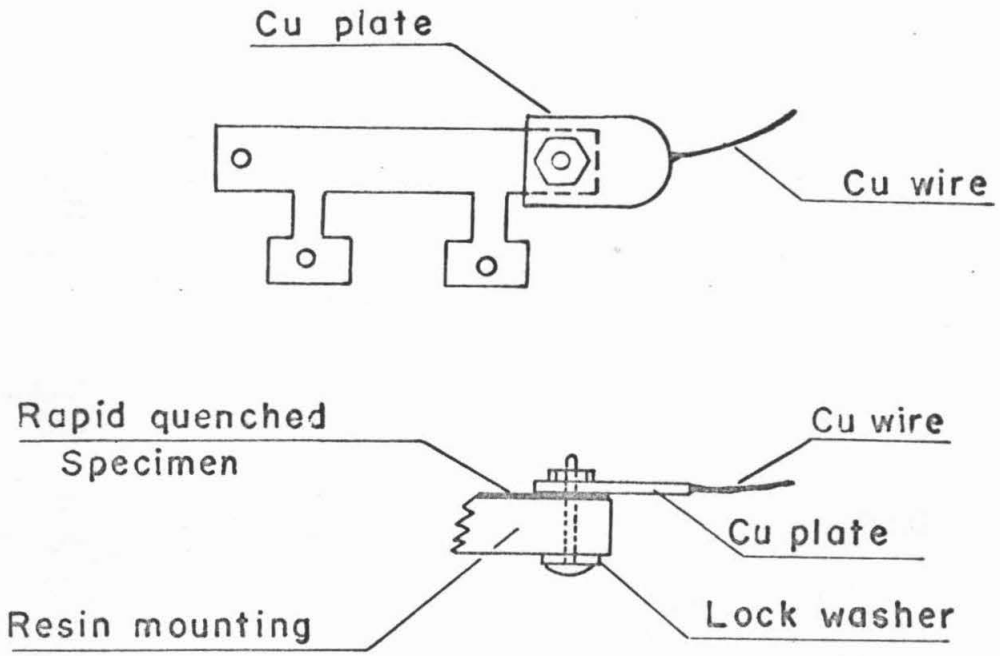

Figure 1. Sample for resistance measurement

diameter. This container with the sample inside is immersed in liquid nitrogen contained in a 6" diameter dewar 11" deep. After the container is in thermal equilibrium with liquid nitrogen, liquid nitrogen is removed from the dewar. Because of the large thermal inertia of the container, the temperature of the specimen increases slowly and steadily in the dewar. Usually the temperature of the specimen increases in such a way that it takes about six hours to cover the temperature range from 77°K to room temperature. This allows ample time to perform resistance measurements while the specimen is in quasi-isothermal condition. Temperature is measured with an uncertainty of ± 0.1°C by using copper constantan thermocouples pressed against the specimen.

Two standard methods of measuring resistance were adopted in this investigation.

a. Potential - current method

This method, which was used for low resistance sample, consists of measuring the small current (0.1 ma) passing through the specimen and the potential drop across the sample. An average value of the potential drop for both directions of current flow is used to minimize any thermoelectric effects..

b. Wheatstone bridge method

This method is used for the specimens of high resistance ($10^3 \sim 10^8$ ohms). The contact resistance can be neglected when it is compared with the sample resistance. A Leeds & Northrup No. 4735 Wheatstone bridge and a Leeds & Northrup No. 2340 galvanometer were

used. No significant thermoelectric effects have been observed when the polarity of the power supply in the bridge circuit is reversed.

The experimental error in resistance measurement is estimated at about 1%.

E. Thermoelectric Power Measurement

Of the three thermoelectric effects, only the Seeback effect has been studied in this investigation, since the thermoelectric power can be measured with relative ease and considerable accuracy. Because the Seeback effect is closely related to the Peltier and Thomson effects by the well-known Kelvin-Onsager relation, complete information on all the thermoelectric properties of a conductor can be derived from a knowledge of the thermoelectric power.

The thermoelectric power may be defined using the circuit shown in Figure 2. If a and b are different conducting materials (perhaps the same material in two different states), an open circuit potential difference is developed as a result of the temperature gradient applied to the thermocouples. Then the thermoelectric power of conductor a with respect to b is defined as

$$S_{ab} = S_a - S_b = \lim_{\Delta T \to 0} \frac{\Delta V_{ab}}{\Delta T} .$$

S_{ab} is conventionally considered as positive if V_{ab} in Figure 2 is positive. The measurement of the thermoelectric power of one conductor against another then consists of establishing a temperature difference ΔT in the thermoelectric circuit in Figure 2 and measuring ΔV and ΔT. The thermoelectric power of various specimens against copper was measured from liquid nitrogen temperature to room

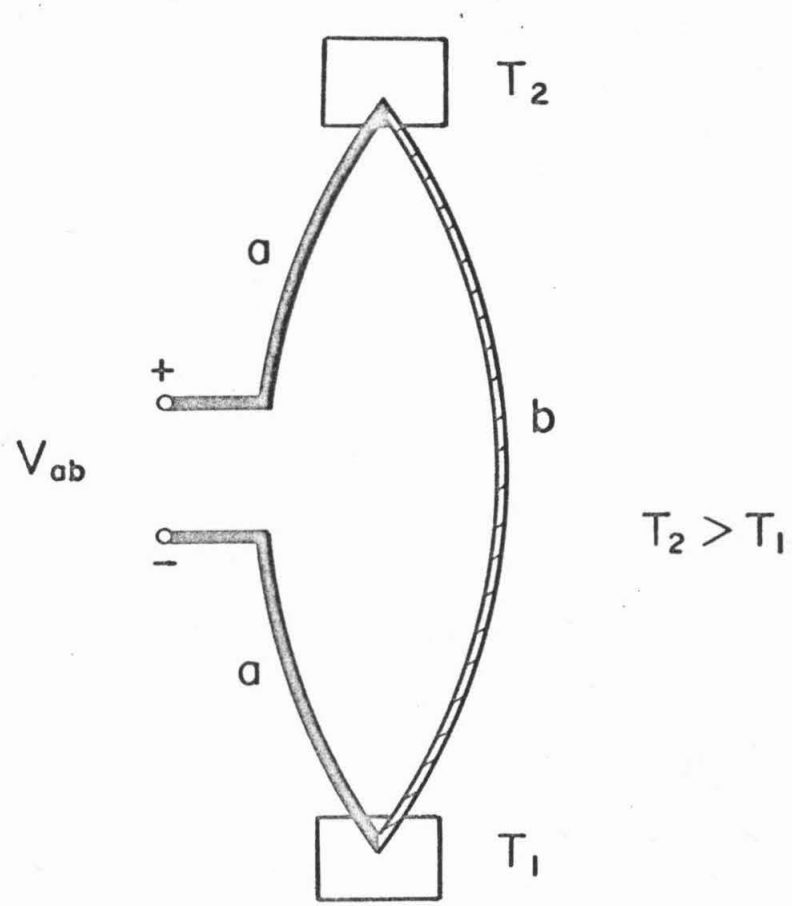

Figure 2. A thermoelectric circuit.

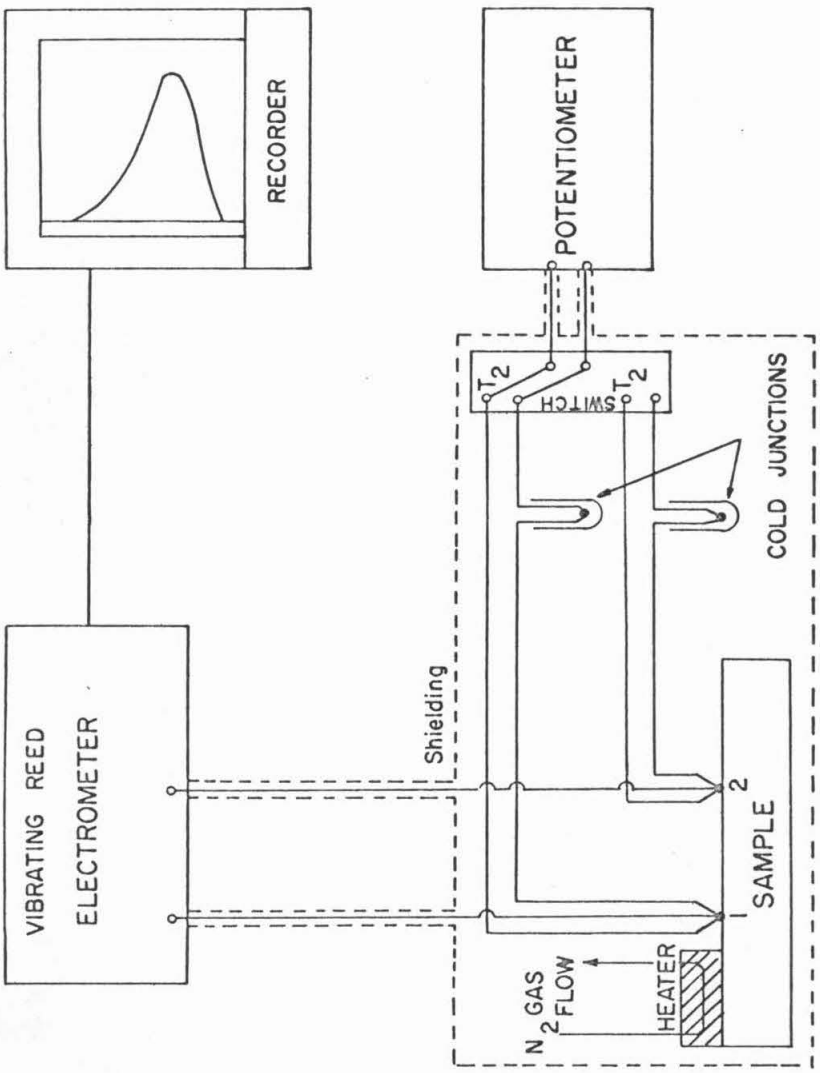

Figure 3. Schematic diagram of the circuit for the measurement of thermoelectric power.

temperature. Then, it is converted to its absolute value since the absolute thermoelectric power of copper is well-known.[7] The specimen to be measured is cooled to liquid nitrogen temperature in a dewar 6" in diameter and 11" in height. Then a temperature gradient is applied to the thermoelectric couple, which consists of copper wire leads and the specimen in question, by passing N_2 gas at room temperature through the heating block pressed against the specimen. The flow rate of N_2 gas controls the temperature gradient and the rate of heating. The temperature difference ΔT which is usually about $8^\circ \sim 10^\circ$ is determined by measuring the junction temperature T_1 and T_2 using copper-constantan thermocouples. The thermal emf produced by this temperature difference is measured with a Leeds & Northrup K-3 type potentiometer when the specimen is of low resistance. The resistance of an amorphous sample at liquid nitrogen temperature is usually of the order of 10^7 ohms. This requires using an electrometer to measure the thermal emf because the conventional galvanometer would have reduced sensitivity for high impedance measurements. Figure 3 shows a schematic arrangement for using a Cary vibrating reed electrometer for thermoelectric measurement. The apparatus used in measuring is shown in Figure 4. Efforts have been made to ensure good electrostatic shielding and high leakage resistance. The specimen 1* to be measured sits on a Teflon table 2. The specimen and

---

*The number refers to the part of the apparatus shown in Figure 4.

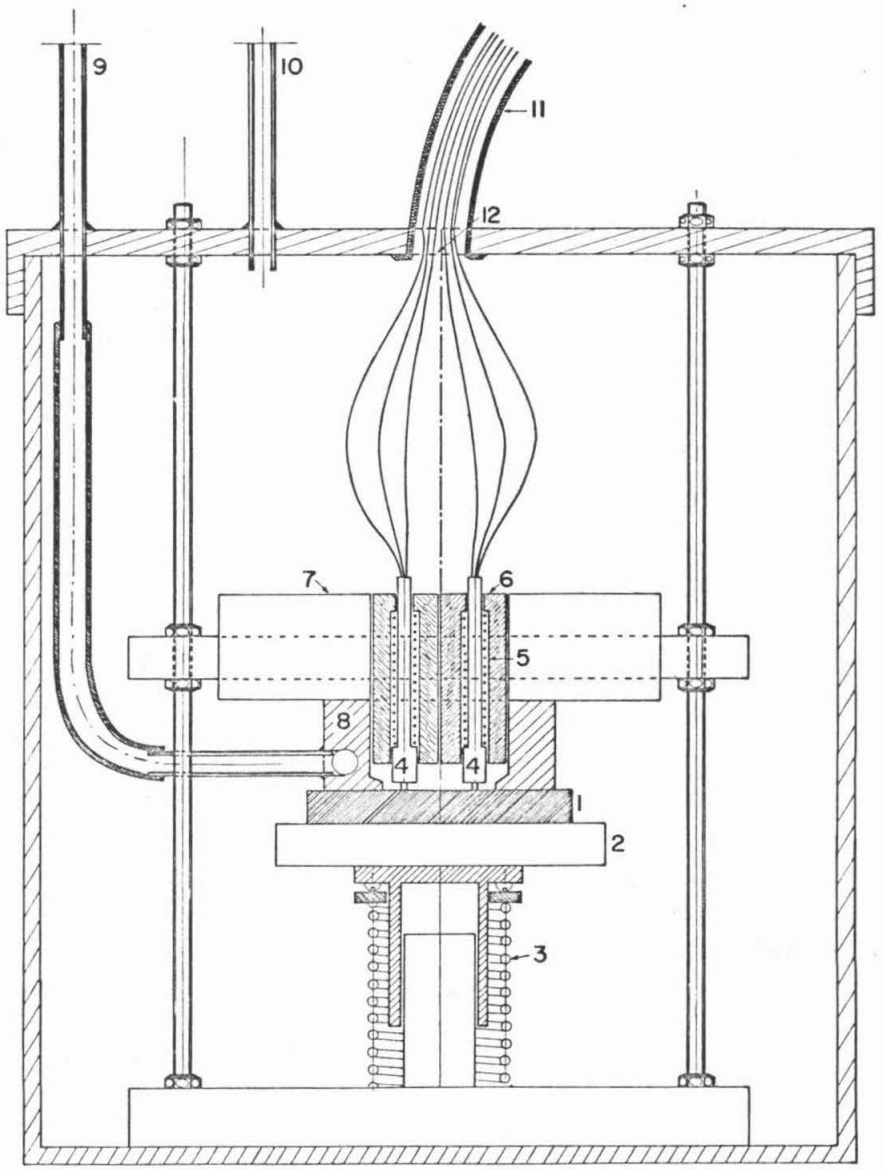

Figure 4. Apparatus for thermoelectric power measurement.

table are pushed against the gas heater 8 which is mounted to 7. Part 4 which is made of Teflon, is used to hold the thermocouple and thermal emf leads. Part 4 is pressed firmly to 1 by the spring 5. Part 6 and 7 are mounted on a horizontal track so that the distance between the two thermocouples can be adjusted by moving them along the track. Part 9 is the inlet of N_2 gas to the heater 8; the outlet is not shown in the diagram. Part 10 is used to keep a very slight N_2 gas flow in order to avoid any water condensation in the apparatus. Part 11 is a coaxial coating for electric shielding purpose.

The thermoelectric power measurement is performed while the specimen is in a quasi-thermal equilibrium as described in the last section. The accuracy of this measurement is about $\pm 2\%$.

III. EXPERIMENTAL RESULTS

A. Metastable Phase Regions Determined by X-Ray Diffraction

In these rapid-quenched alloys two different metastable phases have been detected by X-ray diffraction (Debye-Scherrer method). They are (1) simple cubic phase (2) amorphous phase. Phase regions are shown in Figure 5. It should be remembered that these phase regions are determined within the accuracy of the present experimental conditions. The formation of these metastable phases is a function of the inherent properties of the alloy itself as well as the quenching condition.

B. Lattice Parameter of the Simple Cubic Phase

The lattice parameters of the simple cubic phase described in Figure 5 are determined by the Debye-Scherrer diffraction method at room temperature. The Debye-Scherrer films of the simple cubic alloy are taken in the manner described in Section II. All of the films gave diffuse high angle lines. The wavelength (CuK_α) = 1.54178 Å is used to calculate the lattice parameter. Only alloys which contain 70 atomic percent Te and 30 atomic percent noble metal were measured. Figures 6, 7 and 8 show the lattice parameter of simple cubic alloys versus the atomic percent of copper or silver contained in the alloys. The dimensions of the rectangle box shown in these diagrams indicates the uncertainties in lattice parameter and alloy composition. For the Au-Cu-Te ternary system the lattice parameter decreases at the

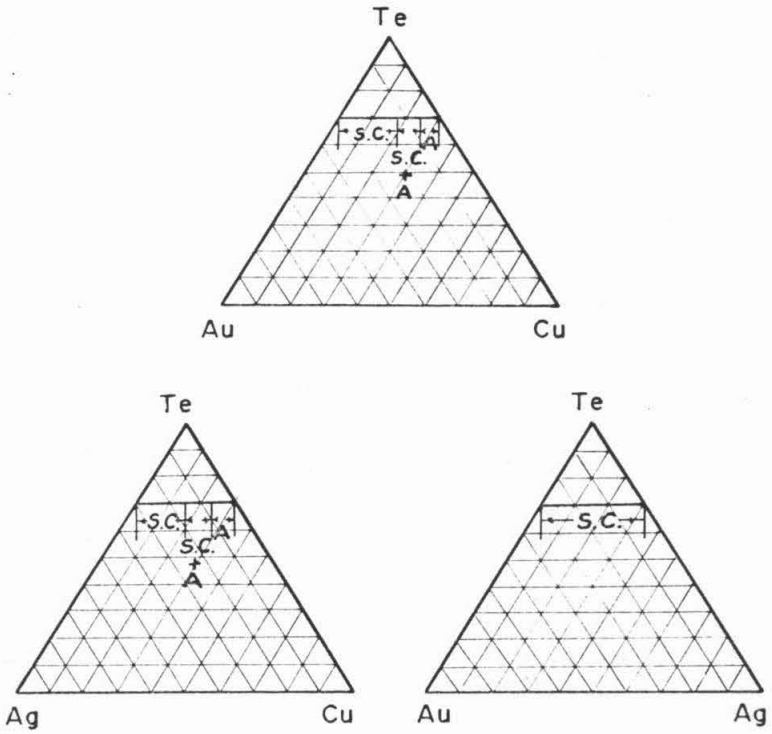

S.C. = SIMPLE CUBIC

A = AMORPHOUS

Figure 5. Metastable phase regions in ternary systems.

beginning as Au atoms are replaced by copper. Then it increases monotonically from about 4.3 at% of Cu thereafter. Thus, for this system the plot of lattice parameter against copper content shows a minimum. The results of lattice parameter measurement of the simple cubic alloys in Ag-Cu-Te system along the constant 70 at. % Te line indicates that there is no detectable effect on the lattice parameter when Ag is substituted by Cu. As shown in Figure 8, the lattice parameter of simple cubic alloys in the Au-Ag-Te system increases with increasing silver content in such a way that it shows a small positive deviation from Vegard's law.

C. Microphotometer Trace of a Typical Amorphous Alloy.

The composition range of the amorphous phase detected in the two Te-base ternary systems has been described in III. A. It is impossible to conduct investigations which cover the whole amorphous range in each system within a reasonably short time. Hence only a typical amorphous alloy which contains 5 at. % Au, 25 at. % Cu and 70 at. % Te was studied extensively. A Debye-Sherrer x-ray diffraction pattern of this alloy was obtained by using MoK_{α} radiation monochromatized by the (200) plane of a lithium fluoride crystal. A microphotometer trace of the film is shown in Figure 9, where the disappearance of constructive interference of x-ray scattering is clearly demonstrated. The tendency of atoms to arrange themselves at a preferred statistical interatomic distance is shown by the three broad maxima centered at $\theta = 6.45^{\circ}$ 10.33°, 16.5° respectively.

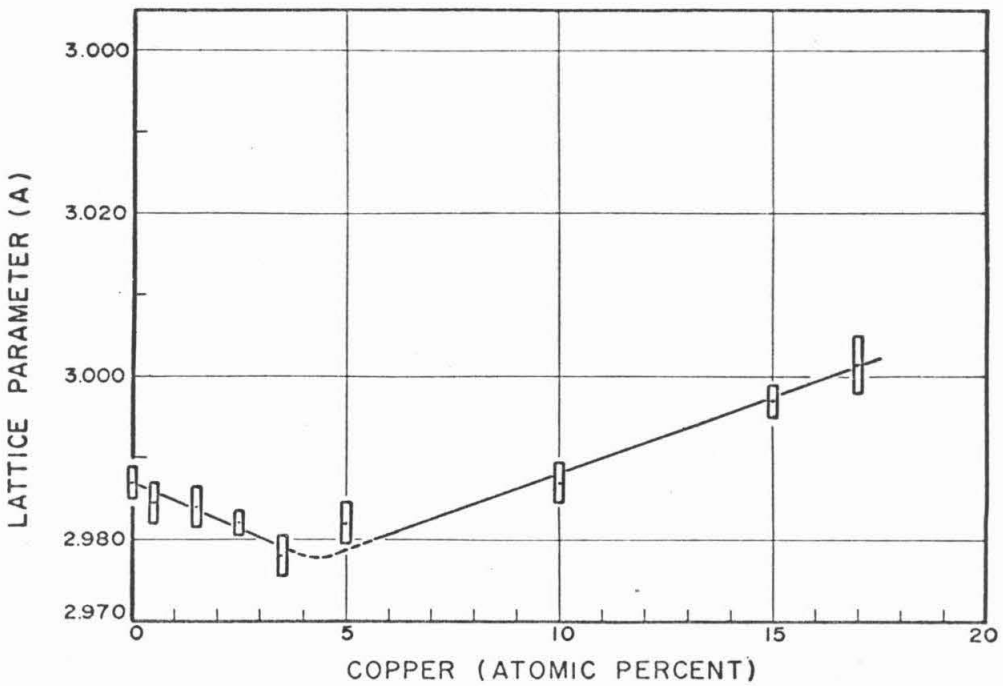

Figure 6. Lattice parameter of the simple cubic alloy containing 70 at. % Te 30 at. % of (Au + Cu).

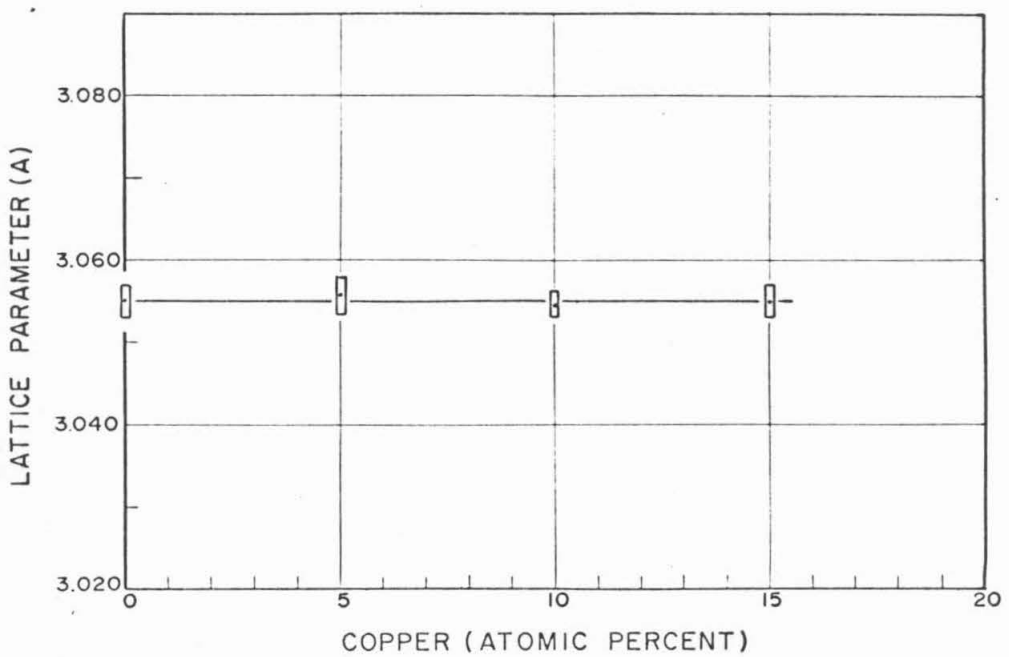

Figure 7. Lattice parameter of the simple cubic alloy containing 70 at. % Te 30 at. % of (Ag + Cu).

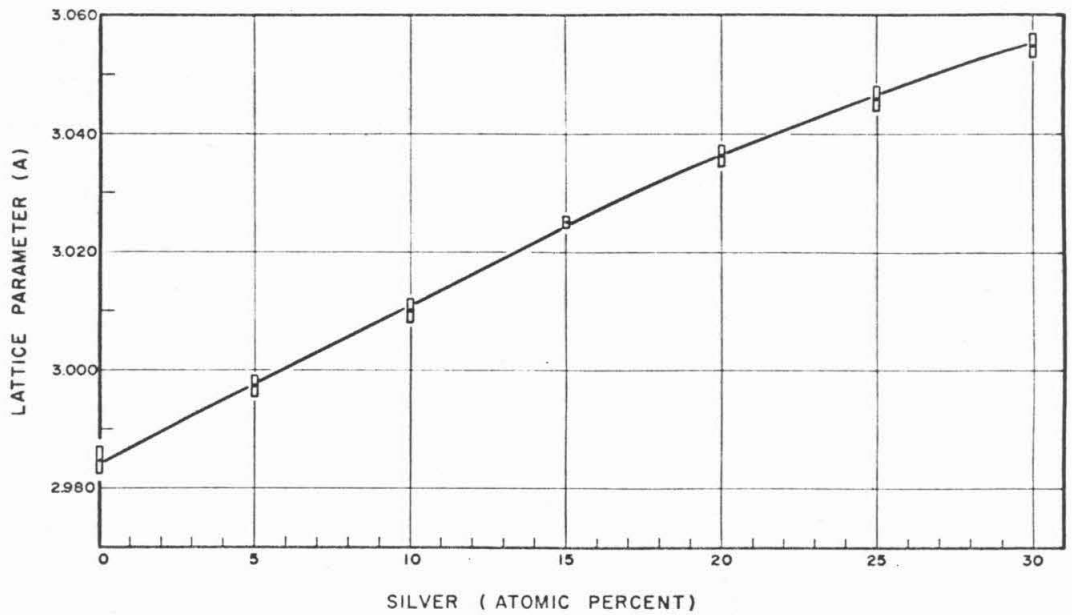

Figure 8. Lattice parameter of the simple cubic alloys containing 70 at. % Te, 30 at. % (Au + Ag).

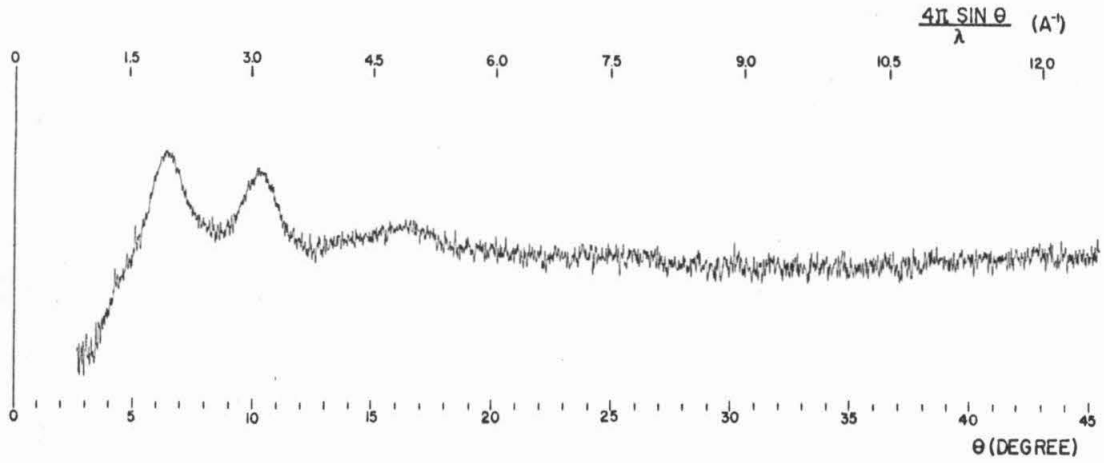

Figure 9. Microphotometric trace of X-ray diffraction patterns for the alloy $Au_5 Cu_{25} Te_{70}$.

D. Results of Resistance Measurement

1. Resistance vs Temperature

a. The resistance vs temperature plot for simple cubic alloys 30 at. % Au, Te; is presented in Figure 10. The estimated resistivity at room temperature is about 10^{-3} Ω-cm. The fact that the electrical resistance of this alloy is a linear function of temperature suggests that it is metallic.

b. The amorphous alloy exhibits a quite different conduction behavior from that of the simple cubic alloy. Its resistance is plotted against reciprocal temperature in Figure 11 which gives two segments of straight line with a broad transition in between. The temperature of the transition region extends from ~120°K to 180°K. In the linear portions of the resistance vs $\frac{1}{T}$ curve the resistance can be expressed by $R = R_o\, e^{E_g/2kT}$ where k is Boltzmann constant, E_g the energy gap in electron-volt, R_o is a constant. The two energy gaps for this amorphous alloy are found to be 0.21 ± 0.01 ev, and 0.09 ± 0.015 ev. The major contribution to the uncertainty in determining the energy gap comes from the difficulty of keeping the quenching condition identical for each sample. There is no significant effect on the temperature dependence of resistance when various amounts (30 ppm ~ 100 ppm) of different impurity atoms (Bi, Sb, Mn, In, Cd) are artificially introduced into the alloy. The absence of impurity effect in amorphous solids will be discussed in the next section. The resistance vs temperature curve of an amorphous sample annealed at 355°K for

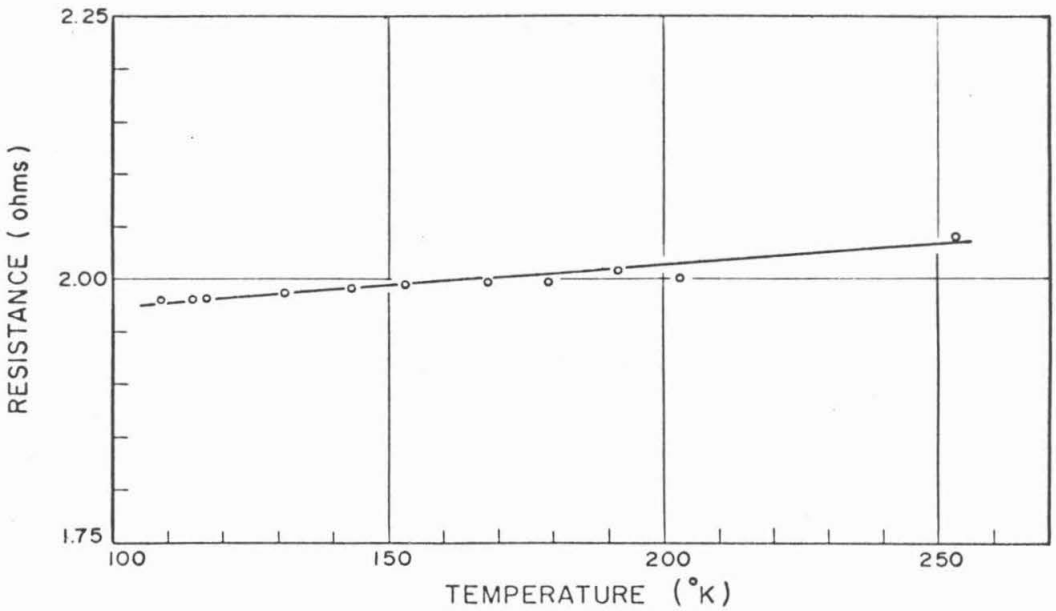

Figure 10. Resistance vs temperature for the simple cubic alloy $Au_{30}Te_{70}$.

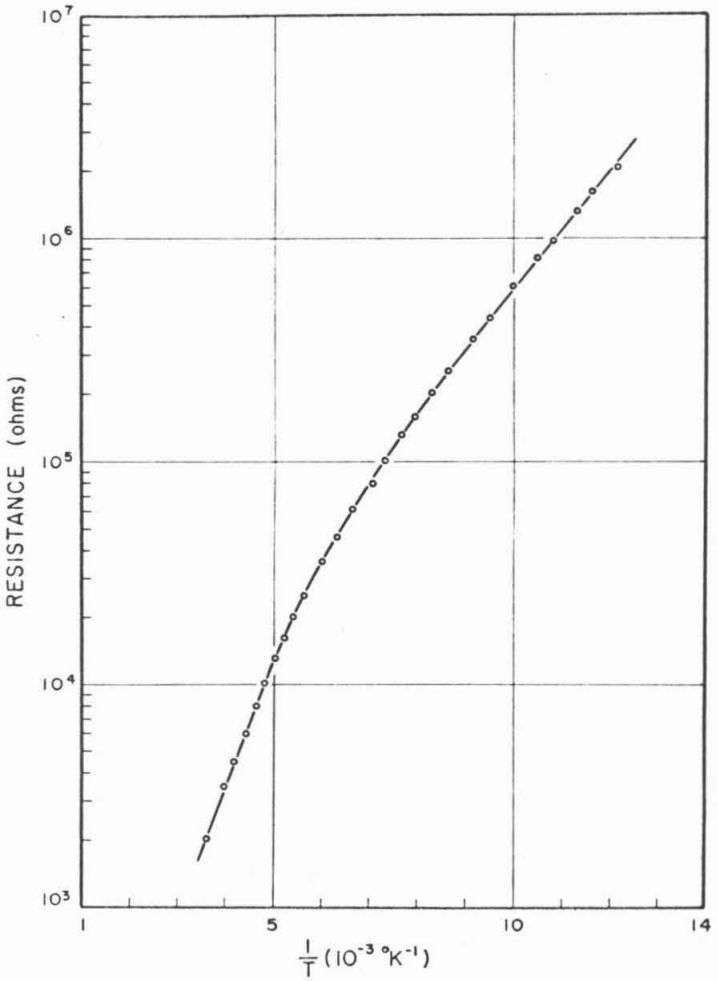

Figure 11. Resistance vs reciprocal temperature for the amorphous alloy $Au_5 Cu_{25} Te_{70}$.

24 hours is shown in Figure 12. As the alloy of the same composition in the equilibrium state, the annealed sample also shows essentially a metallic conduction. The resistance decreases about three orders of magnitude when it transforms from amorphous to crystalline state.

2. Intrinsic Energy Gap vs Concentration

The intrinsic energy gap of the amorphous alloys containing 70 atomic percent tellurium in Au-Cu-Te system has been computed from the resistance versus reciprocal temperature plots. The results are shown in Figure 13 which indicates that the intrinsic energy gap decreases slowly with increasing copper content. The implication of this fact will be discussed in next section.

3. Transformation of the Amorphous Alloy

In order to investigate the metastability of the amorphous alloy, several quenched samples were annealed at various temperatures. The transformation of the metastable phase to equilibrium was followed by measuring the change of resistance. A typical resistance vs annealing time at a constant temperature is shown in Figure 14. The annealing temperature was 353^{o}K. The resistance of the sample decreases slowly at first, then after a period of fast decreasing the decreasing rate slows down and finally reaches its equilibrium value. The plots of time required for a certain amount of transformation versus reciprocal annealing temperature plots are shown in Figure 15. The amount of

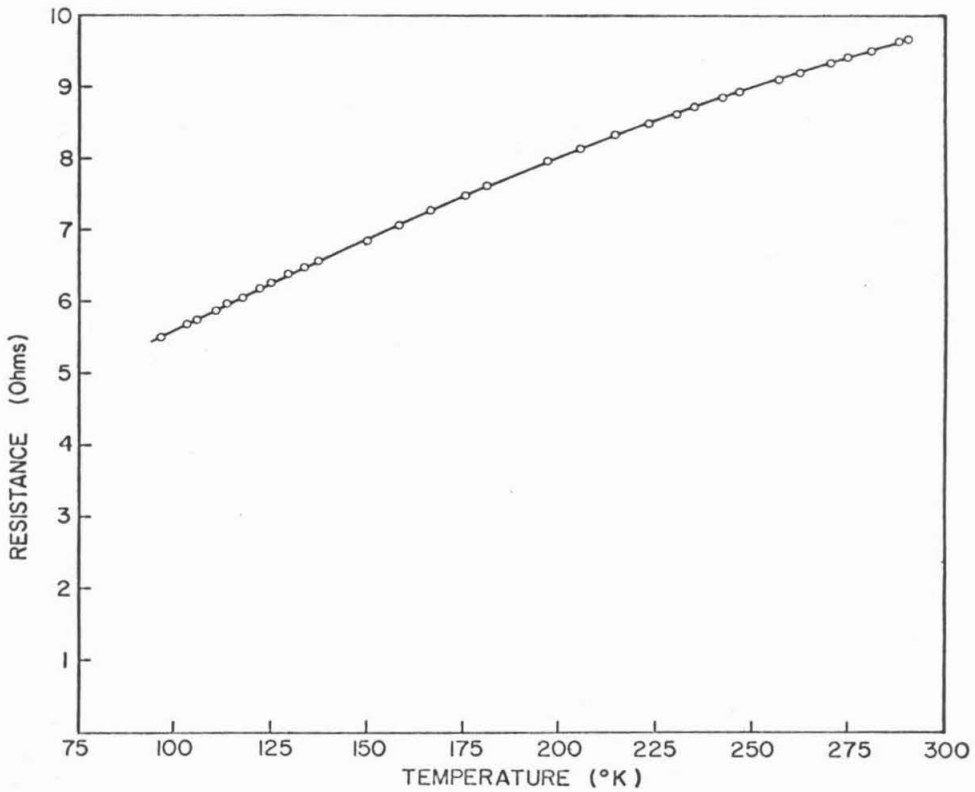

Figure 12. Resistance vs temperature of the amorphous alloy $Au_5 Cu_{25} Te_{70}$ annealed at 355°K for 24 hours.

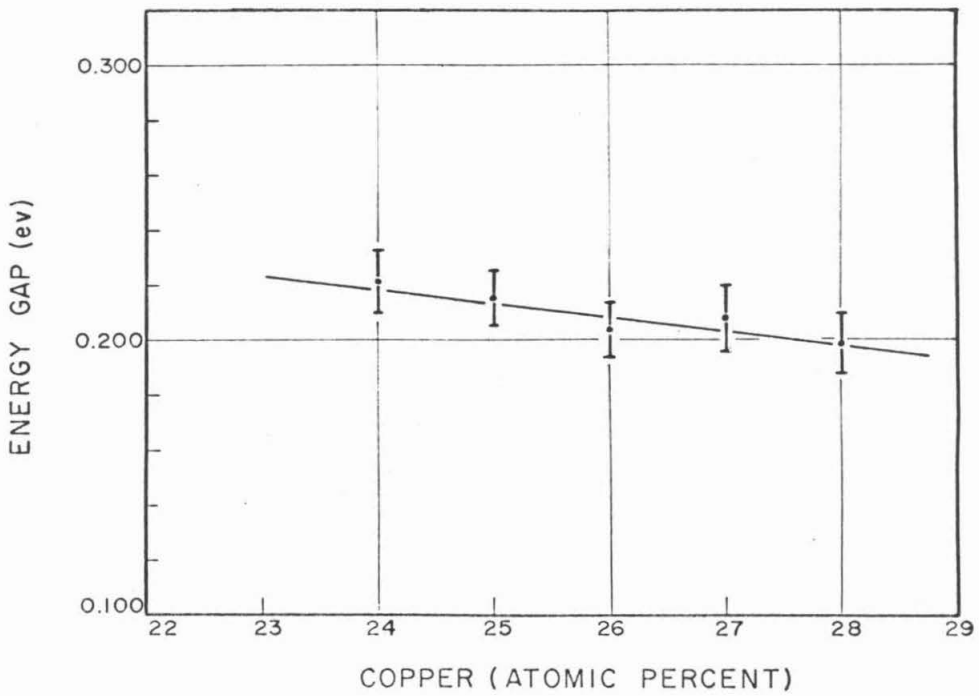

Figure 13. The intrinsic energy gap of the amorphous alloys containing 70 at. % Te 30 at. % (Au + Cu).

transformation is defined as the ratio of the resistance change to the final resistance change, namely $\frac{R_o - R_t}{R_o - R_\infty}$ where R_o is the initial resistance, R_t the resistance at annealing time t, R_∞ the equilibrium resistance. Figure 14 indicates that the transformation is a diffusion-controlled process and the time required t_n for a n percent transformation can be expressed as follows:

$$t_n = A e^{+\frac{Q}{RT}} \qquad (1)$$

where Q is "activation energy", T is absolute temperature, and R the gas constant 1.987 cal/^{o}K-gm-mole). A has the physical significance of being the time required to have a specific amount of transformation at infinite temperature. From Figure 15, Q is computed to be equal to 40,000 cal/gm-mole. By extrapolation, the time needed to have 50% transformation occured at toom temperature is found to be about 2×10^3 days.

E. Thermoelectric Power of the Metastable Phases As a Function of Temperature.

1. The thermoelectric power of the simple cubic $Au_{30}Te_{70}$

The thermoelectric power of the simple cubic alloy $Au_{30}Te_{70}$ is plotted against temperature in Figure 16 which shows the thermoelectric power of this alloy is a linear function of temperature. This agrees with the fact the resistance of this alloy exhibits metallic behavior. The magnitude of the thermoelectric power also falls in

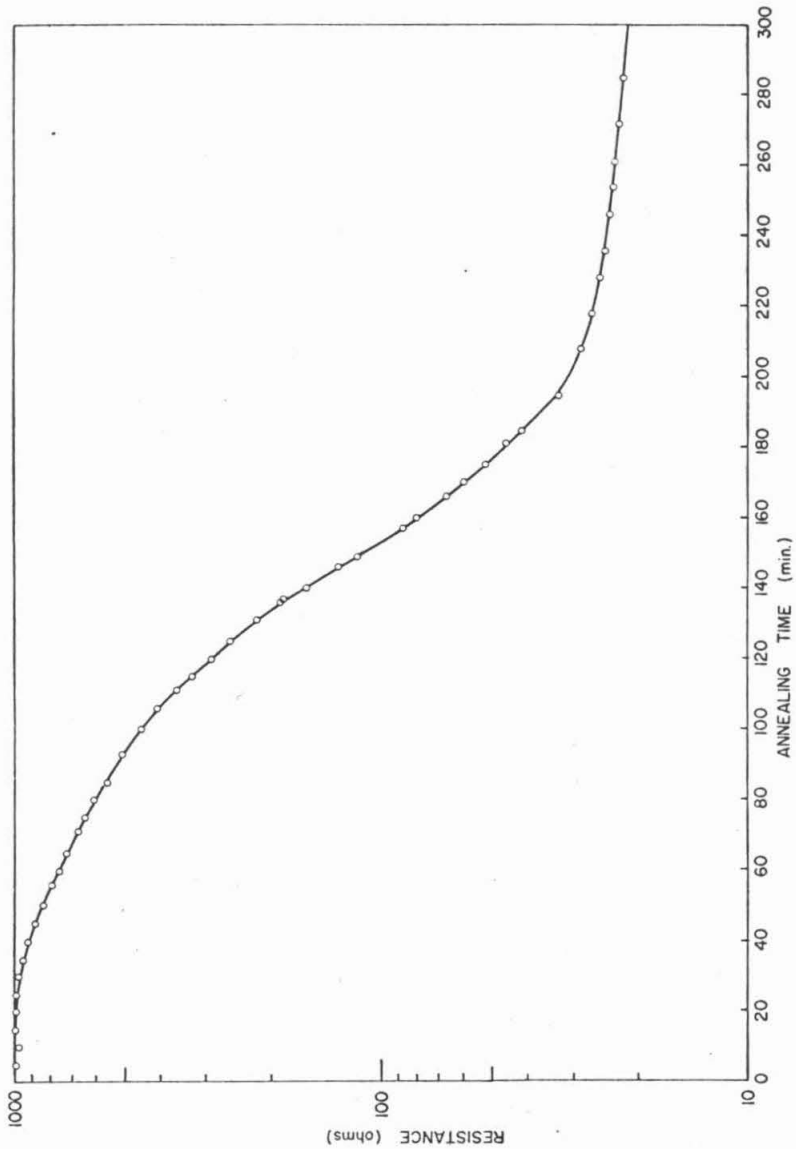

Figure 14. A typical resistance vs annealing time plot for the amorphous alloy $Au_5 Cu_{25} Te_{70}$ annealed at 353°K.

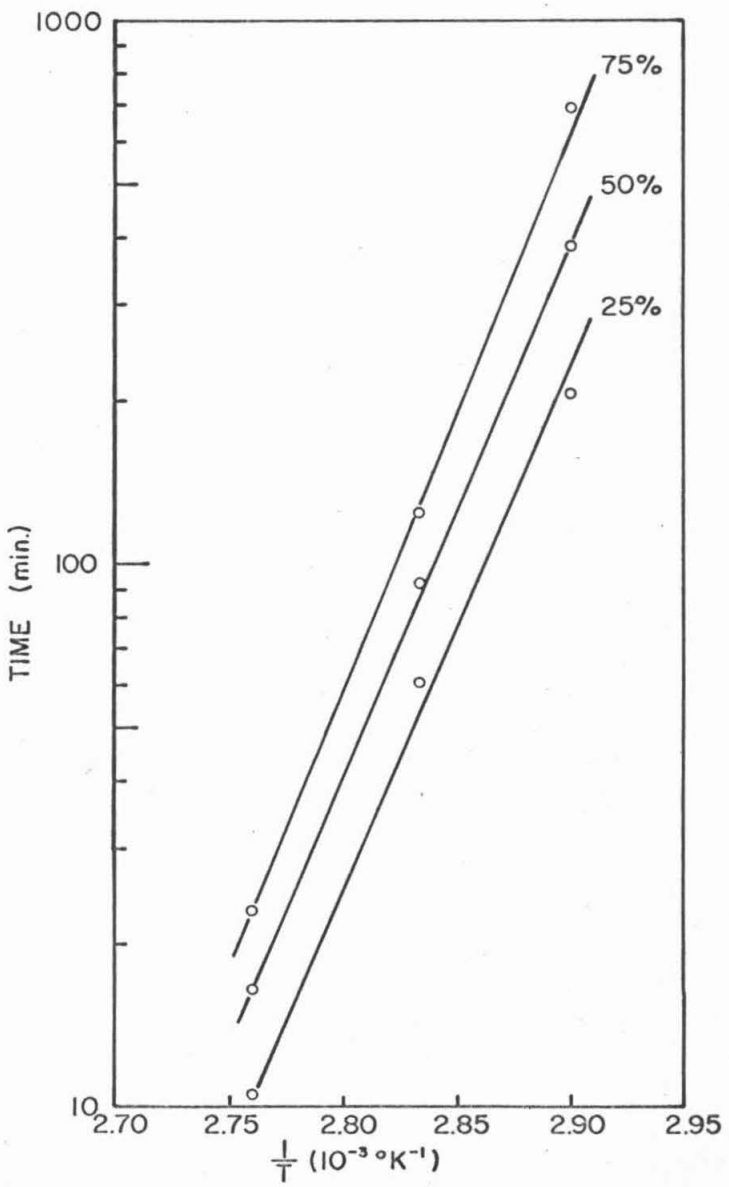

Figure 15. Time for indicated amount transformation vs reciprocal temperature for the amorphous alloy $Au_5 Cu_{25} Te_{70}$.

the range for metallic conductors.

2. The thermoelectric power of the amorphous alloy $Au_5\ Cu_{25}\ Te_{70}$

The thermoelectric power of this amorphous alloy reflects its semiconducting nature. It has a thermoelectric power of about 275 $\mu V/^{o}K$ at $100^{o}K$ and increases steadily up to 335 $\mu V/^{o}K$ at $180^{o}K$ then it decreases slowly to 320 $\mu V/^{o}K$ at room temperature. As in the case of resistance of the annealed sample, the thermoelectric power of the amorphous alloy annealed at $355^{o}K$ for 24 hours is linearly dependent on temperature. The order of magnitude of thermoelectric power of this sample corresponds to that of a metal.

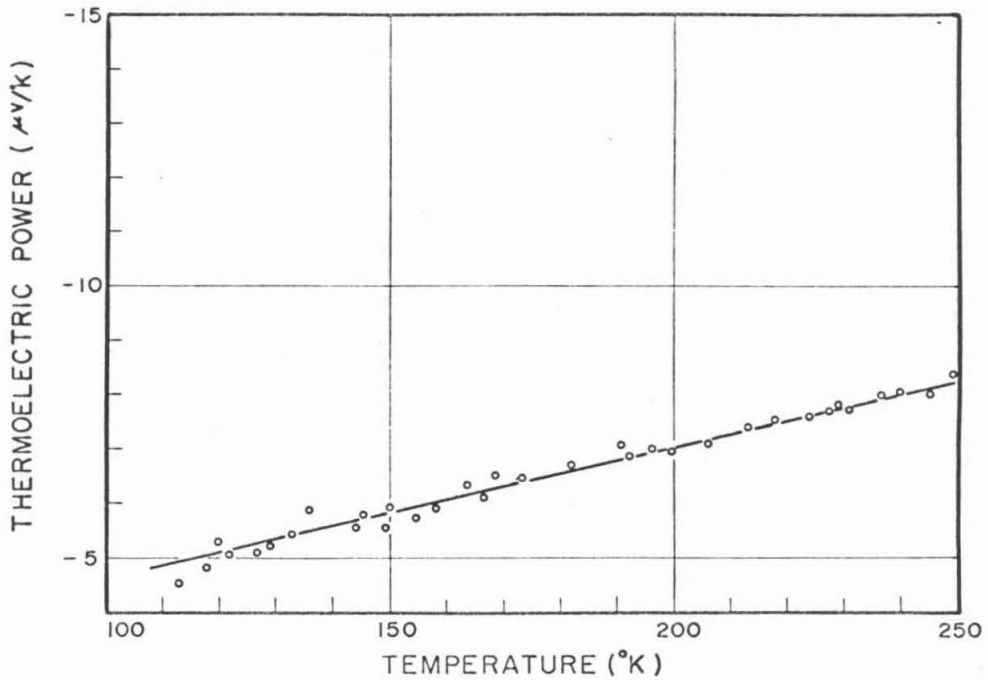

Figure 16. The thermoelectric power of the simple cubic alloy $Au_{30}\ Te_{70}$.

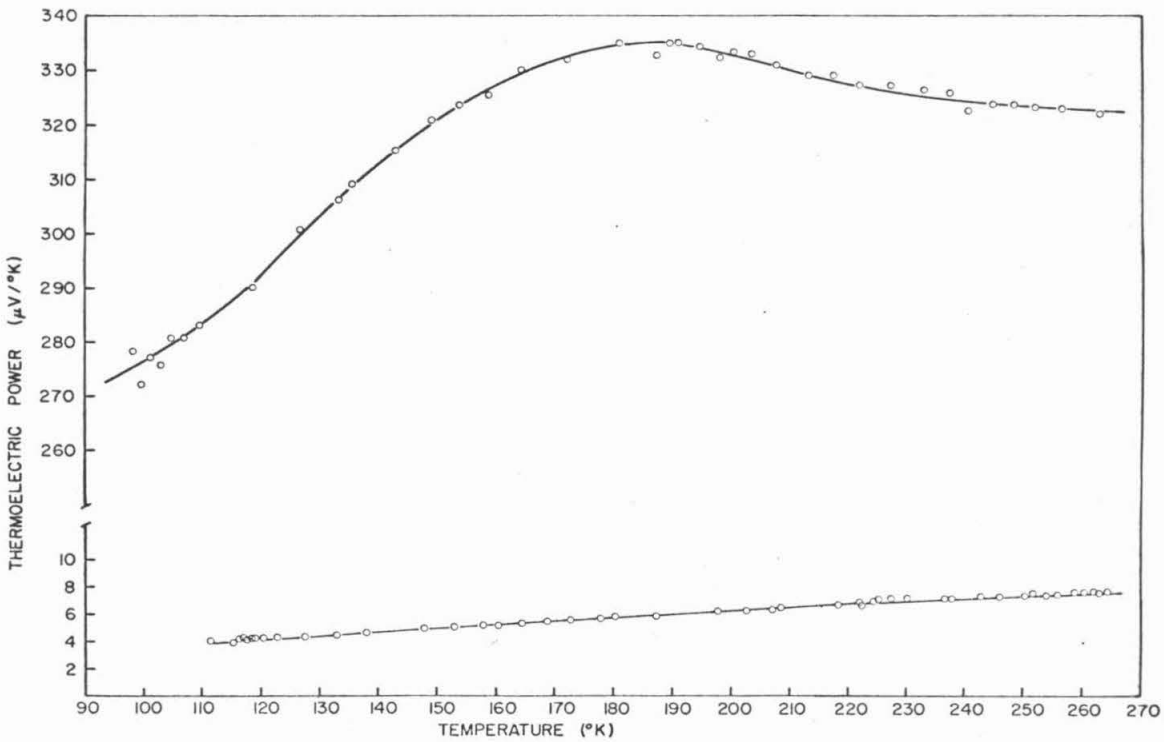

Figure 17. The thermoelectric power of the amorphous alloy $Au_5 Cu_{25} Te_{70}$ (upper curve) and of the same alloy annealed at 355°K for 24 hours.

IV. DISCUSSION

A. The Formation of the Simple Cubic Phase

Since all the alloys investigated in the present work contain 70 at. % of tellurium, it is expected that the crystal structure of pure tellurium is closely related to the structure of the metastable phases obtained in this experiment. Therefore, a brief description of the crystal structure of tellurium is in order.

Tellurium belongs to group VI b of the periodic table. Like the other members of this group, tellurium has six outer electrons, $s^2 p^4$, outside its filled shell. In terms of electtical conductivity, the members of this group vary from insulators (0 and S), through semiconductors (Se and Te) to a metal (Po). Tellurium[8], which has the same crystal structure as selenium, crystallizes in a hexagonal lattice. Associated with each lattice point are three atoms which are arranged in spiral form. That is to say tellurium atoms form spiral chains with three atoms per turn and the axes of these chains are located at the corners of a hexagon. Figure 18 (a) shows the spiral chain structure of tellurium and its important lattice constants. Figure 18 (b) is a top view of the tellurium lattice looking along the three-fold screw axis. It is believed that a given Te atom shares covalent bonds with its two nearest neighbors. The chains are weakly held together by means of van der Waals binding. This combination

(a)

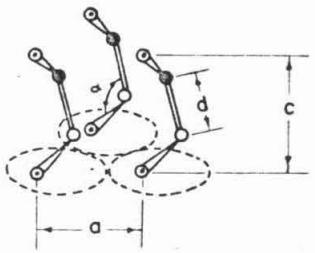

(b)

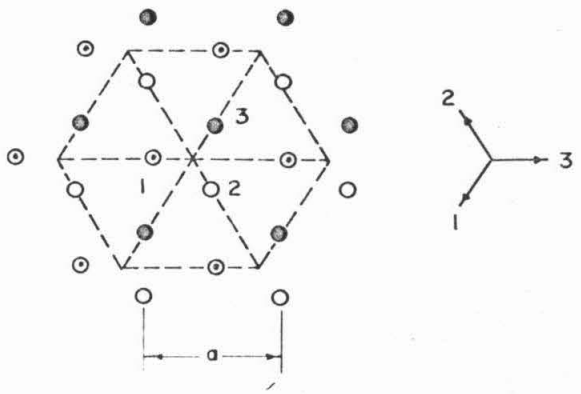

Figure 18. The crystal structure of tellurium
(a) Sketch of the chain structure (after Epstein[9]).
a = 4.45Å; C = 5.92Å; d = 2.86Å; $\alpha = 102.6^{\circ}$

(b) Top view along c-axis, the arrows indicate the the directions of the displacement of the tellurium atoms at different layers to make a simple cubic lattice as shown in Figure 19.

of bindings accounts for the observation that tellurium, unlike most hexagonal structures, cleaves most readily along the (10. 0) plane. Measurements of mechanical properties also seem to indicate that the bonding between the next-nearest-neighbors of adjacent chains is less strong than that between the nearest-neighbors within a single spiral chain.

The simple cubic structure(one atom per unit cell) is interesting in the respect that this crystal structure simplifies theoretical calculation of many properties in solid state theory. Many structures bear a more or less simple relationship to the simple cubic structure. For instance, a body-centered cubic lattice can be considered to contain two identical simple cubic lattices, one consisting of the corner atoms, the other of the center atoms. Furthermore, more complicate structures like that of tellurium and selenium can also be derived from simple cubic lattice. Bradely[8] pointed out the relation between the simple cubic structure and the hexagonal chain structure of tellurium and selenium. In his paper on determining the crystal structure of tellurium and selenium he showed, as in Figure 19 (a), [10] that the displacement of three consecutive planes of the simple cubic lattice along directions which are at 120° to each other produces the structure of tellurium and selenium. Conversely, it is easy to see, from Figure 18 that if the atoms move in the directions indicated, the tellurium structure can be converted into a simple cubic lattice. Namely, after the displacement of tellurium atoms the projection of the Te-lattice along c-axis (Figure 18b) is converted to a top

(a)

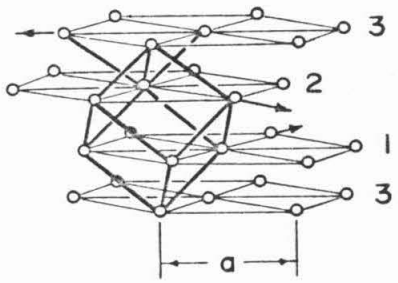

(b)

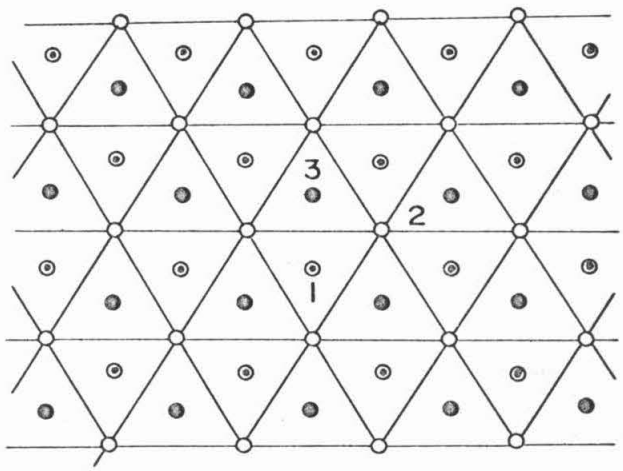

Figure 19. The simple cubic crystal structure
(a) the relation between simple cubic lattice and the tellurium structure (after von Hippel)

(b) top view of a simple cubic lattice along [111].

view of the simple cubic lattice looking along the [111] direction. Since tellurium is a major component of the alloys studied in this experiment, the occurrence of the simple cubic structure in the way described above is possible. The validity of this hypothesis will be examined by comparing the calculated lattice parameter (based on this hypothesis) and the experimental results.

B. The Lattice Parameter of the Simple Cubic Phase

If the theory of the last section is valid it should predict the lattice parameter of simple cubic alloys in fairly good agreement with the experimental values. From Figure 19a it is easy to see that the lattice constant a of hexagonal tellurium is $\sqrt{2}$ times the lattice parameter of the simple cubic Te. Therefore the lattice parameter of a hypothetical simple cubic Te is $4.45\text{Å}/\sqrt{2} = 3.15\text{Å}$. The simple cubic lattice parameters for pure Te extrapolated from metastable simple cubic Te-Au, Te-Ag alloys [2] are 3.15A and 3.07A respectively. These results indicate that the theory is not far from reality. In the case of alloys the effect of noble metals on the lattice parameter is taken into account by making use of the concept of atomic radius. The following is a sample calculation for the alloy which contains 30 at. %Ag, 70 at. %Te. According to L. Pauling [11] the atomic radii of copper, silver, gold and tellurium are 1.276Å, 1.442Å, 1.439Å and 1.60Å respectively, then the equivalent atomic radius of an atom in the alloy (Ag_{30} Te_{70}) is:

$$r_{Ag_{30}Te_{70}} = (0.7 \times 1.60^3 + 0.3 \times 1.442^3)^{\frac{1}{3}} = 1.56 \text{ Å}$$

The simple cubic lattice parameter which corresponds to this alloy is

$$a_{s.c.} = \frac{1}{\sqrt{2}} \times 4.45 \times \frac{1.56}{1.60} = 3.07 \text{ Å}$$

Similar calculations have been performed on other alloys. For comparison the calculated and the experimental results are listed below:

Alloy Composition	Simple cubic lattice parameter (Å) Calculated	Experimental
Te	3.15	3.15 3.07 (extrapolated)
$Ag_{30} Te_{70}$	3.07	3.06
$Au_{30} Te_{70}$	3.07	2.98
$Au_{25} Cu_5 Te_{70}$	3.03	2.98
$Au_{15} Cu_{15} Te_{70}$	3.02	3.00
$Ag_{20} Cu_{10} Te_{70}$	3.04	3.05
$Ag_{20} Au_{10} Te_{70}$	3.07	3.04
$Ag_{10} Au_{20} Te_{70}$	3.07	3.01

In view of the crude assumptions made in the calculation the agreement is satisfactory, but this theory can not account for the detailed variations of the lattice parameter over the range studied. This indicates the simple-minded concept of atomic radius is not sufficient to describe the real situation. With the available experimental information, no satisfactory explanation for the lattice parameter minimum observed in Au-Cu-Te system can be offered at this time. In Ag-Cu-Te ternary alloys, it is found that the simple cubic lattice is not altered when silver is replaced by copper while the tellurium content is kept

at seventy atomic per cent. This experimental finding is consistent with the fact that the equilibrium phase diagrams of Ag-Te and Cu-Te binary systems are homologous (see Appendix).

C. Theoretical Consideration of the Validity of Band Theory in an Amorphous Substance

There are many experimental facts[12] that strongly indicate the existence of amorphous semiconductors, either in the liquid or solid states. The results of resistance and thermoelectric power measurements in this work also clearly show that the amorphous alloy exhibits semiconducting properties in spite of its lack of long-range crystalline order. All these lead one to wonder: What is the basis for the existence of the band structure in the energy spectrum of an amorphous substance which has no long-range order? Is the band theory which is derived from the periodicity of the atomic arrangement still valid in the case of an amorphous conductor? What are the effects on the band structure as a result of the disappearance of long-range crystalline order? Gubanov[13] has proved theoretically that the band structure can exist in an amorphous substance as long as there is short-range order. Several investigators[14], [15] performed numerical calculations on a one-dimensional model of liquid with finite number of atoms. The results of this calculation also indicate the existence of band structure in one-dimensional liquid. The theories will be reviewed briefly for the convenience of subsquent discussions. Gubanov has treated both the one-dimensional and three dimensional cases. For simplicity, the one dimensional amorphous substance is considered here. It is possible

to extend this theory to the three-dimensional case through a relatively cumbersome mathematical manupulation.

In a one-dimensional crystal which consists of a chain of atoms located at equal distances a from one another, the motion of the electrons is governed by the well-known Schrödinger equation:

$$-\frac{\hbar^2}{2m}\frac{d^2\psi}{dx^2} + V(x)\psi = E\psi \qquad (2)$$

where V (x) is a periodic potential with a period a, and E is the energy of the electron. When this one-dimensional crystal is transformed to the amorphous state, it is assumed that the change of the distances between adjacent atoms can be written as $a(1 + \epsilon\gamma)$, where $\epsilon \ll 1$ is a constant parameter which serves as a measure of the degree of disorder and γ is a random quantity which obeys a Gaussian distribution. The assumption that there is no expansion or contraction during the transition from crystalline state to amorphous state requires $\langle\gamma\rangle_{av} = 0$. The normalization of the distribution of γ leads to the condition $\langle\gamma^2\rangle_{av} = 1$. Thus, the distance of the $(N+1)$th atom from the first atom in the amorphous state is equal to $Na + \ell$

$$\ell = \Gamma_n \epsilon a,$$

where Γ_n is the sum of N γ values, $\langle\Gamma_n^2\rangle = N$, $\langle\ell^2\rangle_{av} = \epsilon a N^{\frac{1}{2}}$ If $N > \frac{1}{\epsilon^2}$, then $\langle\ell^2\rangle_{av}$ becomes larger than the lattice constant, i.e. the probability of finding the $(N+1)$th atom is smeared out over a region greater than the lattice constant. Thus the accumulation of small departures from the short-range order leads to a complete distruction of long-range crystalline order at distances $a\epsilon^{-2}$. On transition to the amorphous

state, the periodic potential V(x) is subject to two kinds of modification. First, all the maxima and minima are shifted in horizontal directions (along the x axis) according to the displacement of atoms. Second, the heights of the maxima and minima experience small and random changes as a result of the changes in the distances between neighboring atoms. If the Cartesian coordinate is transformed to a new coordinate ξ which is deformed according to the atomic displacements transition by the following relationship,

$$\frac{d\xi}{dx} = \frac{1}{1+\epsilon\gamma} \tag{3}$$

it is possible to express the potential function V (x) in terms of this new coordinate ξ as follows:

$$V(x) = V_0(\xi) + \epsilon V'(\xi) \tag{4}$$

where $V_0(\xi)$ is periodic in the new coordinate system. $V'(\xi)$ allows for the potential change of the second and is as random as γ, $\langle V'(\xi)\rangle_{av} = 0$.

From eq. (3), it is easy to show that

$$\frac{d^2\psi}{dx^2} = \frac{1}{(1+\epsilon\gamma)^2}\cdot\frac{d^2\psi}{d\xi^2} - \frac{\epsilon}{(1+\epsilon\gamma)^3}\cdot\frac{d\gamma}{d\xi}\cdot\frac{d\psi}{d\xi}$$

or in terms of operators:

$$\frac{d^2}{dx^2} = \frac{d^2}{d\xi^2} - \epsilon\left[2\gamma\frac{d}{d\xi^2} + \frac{d\gamma}{d\xi}\frac{d}{d\xi}\right] + 3\epsilon^2\left[\gamma^2\frac{d^2}{d\xi^2} + \frac{d\gamma}{d\xi}\frac{d}{d\xi}\right] + \cdots \tag{5}$$

Substitute eqs. (4) and (5) into (2), the Schrodinger equation becomes

$$H\psi = E\psi$$

where

$$H = H_0 + \epsilon W + \epsilon^2 w + \cdots\cdots$$

$$H_0 = -\frac{\hbar^2}{2m}\frac{d^2}{d\xi^2} + V_0(\xi), \qquad W = \frac{\hbar^2}{2m}\left[2\gamma\frac{d^2}{d\xi^2} + \frac{d\gamma}{d\xi}\frac{d}{d\xi}\right] + V'(\xi)$$

$$w = -\frac{3\hbar^2}{2m}\left[\gamma^2\frac{d^2}{d\xi^2} + \gamma\frac{d\gamma}{d\xi}\frac{d}{d\xi}\right]$$

H_o can be regarded as the unperturbed Hamiltonian, ϵW and $\epsilon^2 w$ as the perturbations. Since $V_o(\xi)$ is a periodic function, the solution of the unperturbed equation $H_o\psi = E_o\psi$ leads to the familiar energy spectrum consisting of allowed bands separated by forbidden bands. To find out the effect of the perturbations on the unperturbed energy spectrum, perturbation theory has to be used. However, order of magnitude estimation of the perturbation matrix elements indicates that the conventional method of successive approximation is not applicable. Therefore, the relative degeneration method is used to calculate the energy spectrum of the perturbed problem. The following qualitative conclusions can be drawn from this calculation:

(1) As a result of the disappearance of the long-range crystalline order, the energy spectrum of electrons is altered in such a way that allowed bands expand and forbidden bands contract. There is a general upward displacement of both allowed bands and forbidden bands.

(2) Band edges are diffuse, as we would expect from the random disturbances of the short-range order.

(3) As the degree of disorder increases, the forbidden band becomes narrower and narrower and eventually disappears.

The above results remain true when this theory is extended to the three-dimensional case. Makinson and Roberts[15] carried out numerical calculation on a one-dimensional model of liquid similar to the well-known Kronig-Penney model, with equal δ-type potential wells

but distributed according to a cut-off parabolic distribution about the mean value. The length of the chain, usually 2000 atoms, was sufficiently long to ensure the complete destruction of long-range order. By counting the number of nodes of the solutions to the Schrödinger equation in question, it is found that there is a definite energy gap in which no states appear. This energy gap decreases as the degree of disorder increases. Other qualitative results are also in good agreement with Gubanov's conclusions.

From the above discussions, both experiment and theory strongly indicate that long-range order is not a necessary condition for the presence of a band structure. Therefore, it seems reasonable to say that the interactions between neighboring atoms and the atomic distribution which is characterized by the coordination numbers and interatomic distances determine the band structure of a substance no matter whether it is in crystalline or amorphous state. The experimental findings of this investigation will be used to illustrate this idea in the following discussions.

D. The Width of Intrinsic Energy Gap

In order to be able to compare the width of the intrinsic energy gap of the amorphous alloy to that of pure crystalline tellurium a digression to the structure of amorphous alloy is necessary here. The structure of several tellurium-base amorphous alloys obtained by rapid cooling from the liquid state has been studied by x-ray diffraction[16]. It is found that neither the nature of the alloying element nor its con-

centration has a noticeable effect on the shape of the radial distribution function of these amorphous tellurium-base alloys. The average value of the interatomic distances and the coordination numbers of 14 different amorphous tellurium alloys taken from reference (16) are listed in the following table. The interatomic distances and the coordination number of pure crystalline tellurium are also listed for comparison:

	Amorphous Tellurium Base Alloys		Pure Crystalline Tellurium	
nearest neighbor	coordination number	interatomic distance(Å)	coordination number	interatomic distance(Å)
1st	1.8	2.7	2	2.86
2nd	12	4.1	4	3.47
3rd	---	---	6	4.46

From the above table, it is interesting to note the following features about the amorphous alloys:

(1) Amorphous alloys have approximately the same coordination number as that of pure tellurium. The interatomic distance of first nearest neighbors is slightly smaller than that of pure tellurium.

(2) Amorphous alloys have a very large second coordination number 12 compared with the coordination number 4 for crystalline tellurium.

By comparison, it is found that the microphotometer trace of the Debye-Sherrer film for the amorphous alloy Au_5 Cu_{25} Te_{70} (Fig. 9) is almost identical with those of the amorphous tellurium base alloys studied in reference (16). Therefore, it is reasonable to assume the amorphous alloy Au_5 Cu_{25} Te_{70} has a structure very close to the average structure of amorphous base tellurium alloys listed in the table above.

It is generally assumed that in crystalline tellurium, two covalent bonds are formed between the two nearest neighbors. The bonding is associated with the spiral chain parallel to the c-axis in hexagonal tellurium. The tellurium chain structure exists even in the liquid state[17]. Experimentally, it is deduced that there are two nearest neighbors in the amorphous tellurium base alloys. It is therefore hypothesized that the structure of amorphous tellurium base alloys is composed of short and randomly oriented chains of tellurium atoms. Most of the atoms of the alloying element(s) are randomly distributed in the space between tellurium chains and very few of them may occupy the substitutional sites in the chains. In the particular case of the amorphous alloy Au_5 Cu_{25} Te_{70}, most of the copper and gold atoms are distributed between the randomly oriented spiral chains of tellurium, while a very small number of copper and gold atoms occupies the regular sites in the chain substitutionally. The copper and gold atoms may attach to the end of a chain, hence provide a valence electron necessary to form the covalent bond with a tellurium atom. The above hypothesis justifies direct comparison between the intrinsic energy gaps of the

amorphous alloy $Au_5 Cu_{25} Te_{70}$ and pure crystalline tellurium. It also incidentally furnishes a possible explanation for the observation that neither the alloying element nor its concentration has a noticeable effect on the shape of the radial distribution functions of the amorphous tellurium base alloys. Based on this hypothesis, the tellurium atoms form the chain structure. Therefore it is plausible that the minor component of the alloy does not play a significant role on the coordination number and interatomic distances of the first nearest neighbor. However, it can contribute to the coordination number of the second nearest neighbor. Hence, the large second coordination number of the amorphous alloys is explainable under this assumption.

The energy gap of a semiconductor experiences two kinds of change when there is a transformation from the crystalline state to the amorphous state under the condition that the short-range order is not greatly altered. The first kind of change in the intrinsic energy gap is due to the effect of disappearance of long-range order and the small random disturbance of short-range order. According to the two theories mentioned in the last section, this effect always narrows the intrinsic energy gap and is proportional to the degree of disorder. The second change of the energy gap is attributed to the systematic change in the interatomic distance of first nearest neighbors. The sign of this change in energy gap can be either positive or negative depends entirely on the band structure of the individual material and the sign of interatomic distance change. The energy band structure of crystalline tellurium as a function of reduced lattice spacing[18] is shown in Figure 20. It

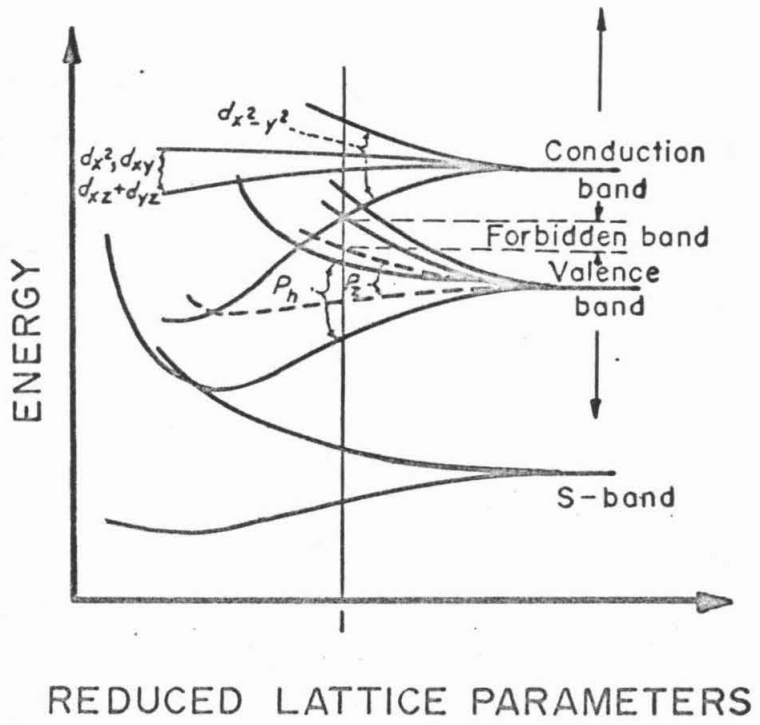

Figure 20. The energy band structure of crystalline tellurium as a function of reduced lattice spacing. (after Gáspár)

shows that the width of forbidden band of tellurium decreases with decreasing lattice spacing. Since in amorphous tellurium-base alloys, the interatomic distance of first nearest neighbor (~2.7 Å) is in general less than that of crystalline tellurium (2.86), the energy gap of amorphous alloys should be smaller than that of tellurium as a result of the smaller interatomic distances. The intrinsic energy gap of crystalline tellurium is found to be 0.34 ev[9] as compared with that of the amorphous alloy $Au_5 Cu_{25} Te_{70}$ 0.21 ev. This reduction in energy gap can be qualitatively interpreted as the result of the two above-mentioned effects.

In the Te-Au-Cu system, the fact that the intrinsic energy gap of alloys containing 70 at. % Te decreases with increasing copper content (Fig. 13) indicates that the degree of disorder increases as more copper atoms replace the gold atoms. This seems to be a logical trend when one considers the fact that the simple cubic phase is gradually changed to an amorphous phase as more copper atoms are present in the alloys.

E. Extrinsic Conduction in Amorphous Solids

Several investigators[4], [19] found no impurity conduction in amorphous semiconductors even when they contain impurity atoms which act as donors or acceptors in crystals with the same chemical composition. These negative observations suggest that in amorphous semiconductors the impurity atoms do not act the same way as they do in crystals and there should be some fundamental reasons behind the absence of impurity conduction in amorphous semiconductors. To find a basis for this experimental fact, Fisher[6] and Gubanov[5] tried to

approach this problem theoretically without getting satisfactory and conclusive result. However, the plot of logarithmic resistance of the amorphous alloy $Au_5 Cu_{25} Te_{70}$ versus reciprocal temperature does show a slope change which usually characterizes the extrinsic conduction in semiconductor. From the slope of linear segment in the lower temperature region, it is found that the extrinsic conduction corresponds to an energy level ~ 0.09 ev above the top edge of the valence band. Since this amorphous alloy has positive thermoelectric power in the temperature range from liquid nitrogen temperature to room temperature, it should be considered as a p-type conductor, and this deep-lying extrinsic energy level acts as an acceptor state. The experimental information available now does not give a clue as to the mechanism which is responsible for this extrinsic conduction. As the doping of several impurities does not alter the conduction of the amorphous alloy significantly, the nature of the extrinsic conduction in the amorphous alloy probably is not of impurity. The hypothesis proposed in the last section permits some speculation on this problem. The copper or gold atoms which occupy a regular site in the tellurium chain, or the end atoms of the chain may represent a big local potential and can give rise to local states which are responsible for this extrinsic conduction. The absence of an impurity effect on the extrinsic conduction of the amorphous alloy is tentatively explained as follows: In accordance with the hypothesis, the structure of the amorphous alloy is quite loose, so the space between the randomly oriented chains can easily accommodate the impurity atoms without producing significant variation in the local potential larger than

that caused by the fluctuation of the atomic distribution. Another possibility is that the local energy states created by large fluctuations of atomic arrangement in the amorphous alloy capture electrons or holes and neutralize the donors or acceptors, causing the absence of impurity conduction.

F. The Resistance and the Thermoelectric Power of the Simple Cubic Alloy Au_{30} Te_{70}

The temperature dependence and the order of magnitude of the resistivity and the thermoelectric power of the simple cubic alloy Au_{30} Te_{70} suggest that this simple cubic alloy behaves like a metal. The tellurium atoms have six outer electrons (s^2 p^4) beyond the closed shells. Two of these electrons are paired in the s-orbital, two in one of the three p-orbitals, while the remaining two are available for covalent bonding in half-filled p-orbitals[10]. In crystalline tellurium, the atoms arrange themselves in spiral chains. Each tellurium atom forms two covalent bonds with its two nearest neighbors. In tellurium-base amorphous alloys, the coordination number and interatomic distance are preserved and the chain structure persist. Therefore, the amorphous alloys exhibit semiconducting properties which are similar to that of crystalline tellurium. However, the situation in the simple cubic alloys is different from that in the amorphous alloys. The chain structure does not exist in the simple cubic lattice. The coordination number is six instead of two, giving approximately 0.57 electrons per bond. Therefore, it is considered that an important part of the binding energy of the simple cubic alloy results from the mutual sharing of the unpaired electrons.

As a consequence of this unsaturated covalent bonding, electrons can move with ease from one atom to another and hence give rise to the metallic conduction.

G. The Thermoelectric Power of the Amorphous Alloy

As shown in Fig. 17, the thermoelectric power of the amorphous alloy $Au_5\ Cu_{25}\ Te_{70}$ increases with increasing temperature in the extrinsic range and decreases slowly with increasing temperature in the intrinsic range. This experimental fact can be qualitatively explained as follows:

A theoretical expression for the thermoelectric power S can be derived by the use of the Boltzmann transport equations which gives the electrical and thermal current densities. The thermoelectric power of a semiconductor is found[20] by evaluating the Thomson coefficient σ_T from electrical and thermal current densities and then integrating the Kelvin-Onsager relation $\sigma_T = T\frac{dS}{dT}$.

In the extrinsic range, only holes (in the case of p type semiconductors) are predominant. Without considering the scattering mechanism of holes, we assume the relaxation time τ is proportional to energy E^b. Then, the thermoelectric power of holes can be expressed as:

$$S_h = \frac{k}{e}\left[\frac{5}{2} + b - \frac{E_F}{kT}\right] \qquad (6)$$

where k is the Boltzmann constant, e the magnitude of electron charge, E_F is the Fermi energy. Eq. (6) shows that in the extrinsic range of temperatures the thermoelectric power should decrease with decreasing

temperature. This conclusion seems to be in qualitative agreement with the experimental result.

In the intrinsic range, the temperature is high enough to justify the neglecting of the extrinsic conducting effect. The number of electrons in the conduction band is equal to the number of holes in the valence band. Both electrons and holes contribute to thermoelectric power in the intrinsic range of temperature. Assume that in this temperature range the phonon scattering is the most important scattering mechanism. The thermoelectric power of a p-type semiconductor is found [20] as follows:

$$S = \frac{k}{e} \frac{\left(\frac{\mu_e}{\mu_h} - 1\right)}{\left(\frac{\mu_e}{\mu_h} + 1\right)} \left(\frac{E_G}{2kT} + 2\right) \qquad (7)$$

where $\frac{\mu_e}{\mu_h}$ = the ratio of mobility of electrons to that of holes, E_G the intrinsic energy gap. Eq. (7) shows that the thermoelectric power should in general decrease with increasing temperature. This equation yields a qualitative explanation of the experimental result in the intrinsic range. The ratio $\frac{\mu_e}{\mu_h}$ of the amorphous alloy remains to be determined experimentally. As a first approximation, let us assume it is equal to that of crystalline tellurium[21], then $\frac{\mu_e}{\mu_h} \sim 2.1$. The intrinsic energy gap for the amorphous alloy is approximately 0.21 ev. When these quantities are substituted into eq. (7), it is found the thermoelectric power of the amorphous alloy is about 200 $\mu V/^{o}K$ which is the right order of magnitude.

From the above discussion, the thermoelectric power of the amorphous alloy confirms the existence of the extrinsic conduction shown by the resistance measurement.

V. Conclusions

(1) The simple cubic alloy Au_{30} Te_{70} is metallic. Its metallic state can be interpreted as a result of unsaturated covalent bonding.

(2) The amorphous alloy Au_5 Cu_{25} Te_{70} is a semiconductor. The resistance measurement of this alloy shows the existence of extrinsic conduction in an amorphous conductor. The thermoelectric power of this alloy is consistent with the results of resistance measurements.

(3) The applicability of the band theory goes far beyond the limits imposed by the periodicity of atomic arrangement from which it was deduced. Long-range crystalline order is not a necessary condition for the existence of a band structure. The interactions between neighboring atoms which are characterized by the coordination numbers and the interatomic distances determine the band structure of a substance no matter whether it is in the crystalline or amorphous state.

REFERENCES

(1) Pol Duwez and R. H. Willens, Trans. A. I. M. E., 227, 362-365 (1962).

(2) H. L. Luo and W. Klement, J. Chem. Phys., 36 1870-1874 (1962).

(3) H. L. Luo and Pol Duwez, App. Phys. Letters, 2, 21 (1963).

(4) T. N. Vengel and B. T. Kolomiets, Soviet Phys. Tech. Phys., 2, 2314-2319 (1957).

(5) A. I. Gubanov, Soviet Phys. -Solid State, 3, 1694-1697 (1961).

(6) I. Z. Fisher, Soviet Phys. -Solid State, 1, 171-173 (1959).

(7) N. Cusack and P. Kendall, Proc. Phys. Soc., 72, 898-901 (1958).

(8) A. J. Bradley, Phil. Mag., 48, 477-496, (1924).

(9) A. S. Epstein, H. Fritzsche, and Lark-Horovitz, Phys. Rev., 107, 412-419, (1957).

(10) A. von Hippel, J. Chem. Phys., 16 372-380, (1948).

(11) L. Pauling, The Nature of the Chemical Bond (Cornell University Press, 3rd ed.), (1960).

(12) A. F. Ioffe and A. R. Regel, Progress in Semiconductors, 4, 237-291, (1960).

(13) A. I. Gubanov, Quantum Electron Theory of Amorphous Conductors, (Consultants Bureau, N. Y.) 1965.

(14) R. Landauer and J. C. Helland, J. Chem. Phys., 22, 1655-1665, (1954).

(15) R. E. B. Makinson and A. P. Roberts, Australian J. Phys., 13, 437-445 (1960).

(16) H. L. Luo, Ph. D. Thesis, California Institute of Technology, (1964).

(17) R. Buschert, I. G. Geib, and K. Lark-Horovitz, Phys. Rev., 98, 1157 (1955).

(18) Gaspar, R., Acta Phys. Acad. Sci. Hung. 7, 289-311 (1956).

(19) B. T. Kolomiets and T. F. Nasarova, Soviet Phys. -Solid State, 2, 159-160, (1960).

(20) V. A. Johnson and K. Lark-Horovitz, Phys. Rev., 92, 226-232, (1953).

(21) S. Tanuma, Sci. Rep. Res. Inst. Tohoku University Ser. A6, 160-171 (1954).

(22) M. Hansen, Constitution of Binary Alloys (1958).

APPENDIX

Equillibrium phase diagrams of Cu-Te, Ag-Te, and Au-Te systems.

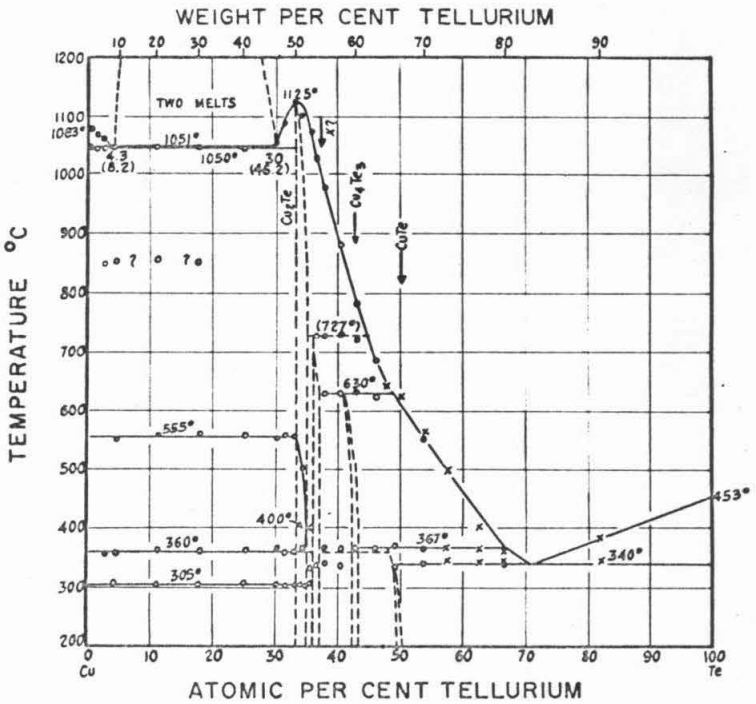

Figure 21. Equilibrium phase diagram of Cu-Te System (after Hansen)(22)

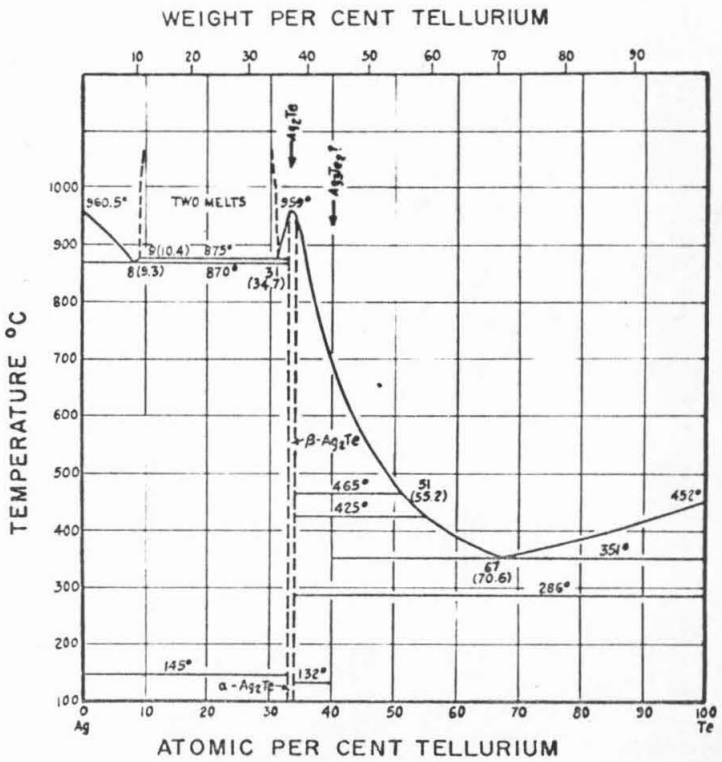

Figure 22. Equilibrium phase diagram of Ag-Te system (after Hansen)[22]

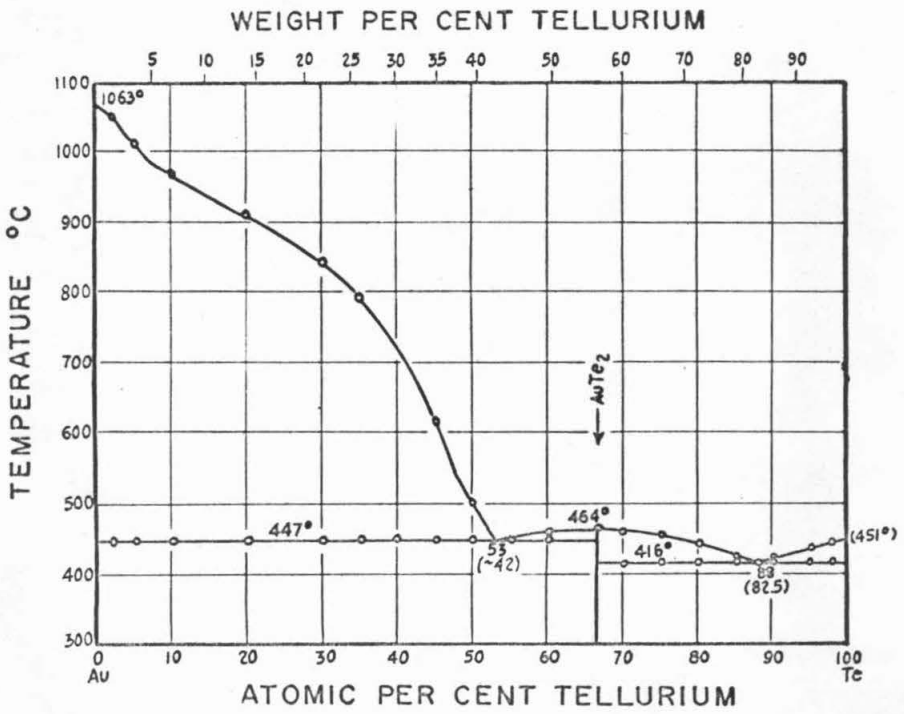

Figure 23. Equilibrium phase diagram of Au-Te system (after Hansen)[22]